THE JOURNAL OF PHYSICAL CHEMISTRY C

Article

pubs.acs.org/JPCC

Surface Reactivity Control of a Borosilicate Glass Using Thermal Poling

A. Lepicard,[†,‡] T. Cardinal,[§] E. Fargin,[§] F. Adamietz,[†] V. Rodriguez,[†] K. Richardson,[‡] and M. Dussauze*[,†]

[†]Institut des Sciences Moléculaires, UMR 5255 CNRS, 351 Cours de la Libération, Université de Bordeaux, 33405 Talence Cedex, France

[‡]Department of Materials Science and Engineering, College of Optics and Photonics, University of Central Florida, Orlando, Florida 32816, United States

[§]Institut de Chimie de la Matière Condensée de Bordeaux, UPR 9048 CRNS, Université de Bordeaux, 87 avenue du Dr. Albert Schweitzer, 33600 Pessac Cedex, France

ABSTRACT: The ability to control glass surface reactivity at different length enables key properties required for future "smart substrates". Employing a thermal poling process on a specific borosilicate glass composition can yield a surface with tailored physical and chemical properties. This work shows that during poling, alkali contained in the glass matrix migrates from the anode to the cathode side of the specimen, yielding the formation of an alkali-depleted layer under the anode. We have shown that this process is responsible for structural changes in the glass network and the formation of a frozen electric field within the glass. Network reorganization is linked to the creation of $BØ_3$ units, which replace $BØ_4^-$ entities upon migration of the alkali ions. The resulting newly charged borate structure leads to a measurable change in the glass' affinity to atmospheric water, being attracted to the poled anodic zone. Such spatial control of surface hydrophilicity can aid in the creation of tailored surface functionality.

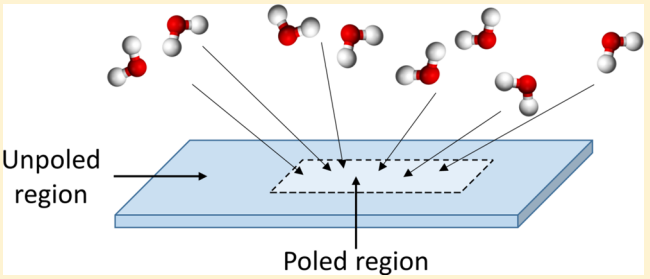

1. INTRODUCTION

In domains such as nano-/biotechnology or lab-on-a-chip, the ability to engineer and control surface properties defines the ultimate function of a surface, in its eventual system use. For this type of application, an ideal substrate should have tunable surface reactivity at a micrometric length scale. Such tunable reactivity is especially useful when associated with detection techniques that access surface information, that is, via optical methods. A perfect material to develop a smart substrate that meets these requirements is optical glass. A glass substrate on which a chemical reaction can take place in a spatially defined area that is integrated with an optical circuit to probe that reaction would be extremely useful. To create such a substrate material, specific tools are necessary to tailor the glass surface properties.

Thermal poling has been used as a structural modification tool, which allows the centrosymmetry of glasses to be broken by the action of a strong electric field. This process, first reported by Myers et al. in 1991,[1] allows for the formation of a second-order nonlinear (SONL) response, usually forbidden in centrosymmetric media such as glasses. The SONL response is defined by an electro-optical effect, described as electric field induced second harmonic generation (EFISH), whereby a static electric field present at the near-anode surface interacts with the third-order optical susceptibility of the glass allowing for the formation of a second-order nonlinear susceptibility. One can describe the effect as follows:[2]

$$\chi^{(2)} = 3\chi^{(3)}E_{(\mathrm{stat})} \quad (1)$$

where $\chi^{(2)}$ and $\chi^{(3)}$ represent the second- and third-order nonlinear susceptibilities, respectively, and $E_{(\mathrm{stat})}$ denotes the strength of the "frozen" induced electric field.

During the poling process, migration of mobile species (alkali ions) from the anode side of the glass toward the cathode occurs. An alkali-depleted layer is left underneath the anode where the presence of the "frozen electric field"[3,4] is established. The induced electric field can approach values near the breakdown voltage of glass, that is, 0.1−1 GV/m.[1] Cation migration also leads to a requisite charge compensation process within the glass matrix. The nature of the electrode, whether blocking or open, influences the compensation mechanism taking place. In the case of an open electrode, typically seen for poling performed in air, charge compensation takes place through injection of hydroxyl groups in the glass and by reorganization of the glass network. In the case of a blocking electrode (such as in vacuum or inert environments), charge compensation can only take place through displacement of negative charge carriers originating from the glass network.[5,6]

Structural changes induced by thermal poling have been well studied in oxide glasses such as in studies of soda-lime,[5] sodium

Received: July 23, 2015
Revised: September 8, 2015

DOI: 10.1021/acs.jpcc.5b07139
J. Phys. Chem. C XXXX, XXX, XXX−XXX

niobium-germanate,[7] borophosphate niobium,[8−10] barium boroaluminosilicate,[11] sodium alumino-phosphate,[12] and borosilicate[13] glasses.

In addition to the modification of structure and induced nonlinear properties, thermal poling has been used as a tool to create glasses with unique surface properties. This interesting possibility has been mainly investigated in bioglasses. Here, alkali-rich glasses typically made of SiO_2, CaO, Na_2O, and P_2O_5 such as those first developed in the late 1960s by Hench[14] are used as glasses that can be incorporated into a body to replace damaged tissues among other uses. These glasses have been found to be good compositions for thermal poling due to their high content of alkali and alkaline either ions.[15] The presence of a strong electric field in a biomaterial has been suggested as a possible way to increase bone growth and bonding mechanism in glasses and ceramics inside a body.[16−20] Thus, in carefully selected glass compositions, it is possible to induce a strong electric field, to locally change the structure of the glass enabling new functionality and properties amenable to a diverse range of applications.

In the present study, we focus on the local modification of the reactivity of borosilicate glasses via thermal poling. In the chosen composition, we try to improve the affinity of the glass toward water. The studied glass resides within a region characterized as part of the boric oxide anomaly, as evident in borosilicate glasses possessing a ratio where $R = Na_2O/B_2O_3$ equals 0.2. In such glasses, it is believed that most of the glass' sodium exists near the borate network and forms charged $BØ_4^-$ structures (with Ø denoting an oxygen bridging two network formers). The silica network is entirely reticulated, as nonbridging oxygens (NBOs) would only form for higher sodium content.[21] The structural changes and corresponding physical changes imparted to the glass during the thermal poling and its repercussions on the glass reactivity in air have been studied using infrared and Raman spectroscopy. The presence of the electric field and its evolution after poling were evaluated and characterized using μSHG imaging. The structural evolution and mechanism associated with the resulting modification are discussed.

2. EXPERIMENTAL SECTION

2.1. Glass Synthesis. Bulk glass with composition SiO_2 39%, B_2O_3 51%, and Na_2O 10% was prepared from high-purity materials, SiO_2 (Sigma-Aldrich, 99,99%), Na_2CO_3 (Sigma-Aldrich, 99.95), and H_3BO_3 (Alfa Aesar, 99.9995%). Raw materials were batched, mixed, ground, and placed into a platinum crucible. The batch was melted at 1100 °C and quenched by dipping the bottom of the crucible in water. The glass was reground and melted again yielding a homogeneous glass. The melt was quenched by pouring the liquid between two brass plates to minimize phase separation. The glass was annealed overnight 40 °C below the glass transition temperature (~450 °C). One millimeter thick samples were then cut and optically polished on both sides. The glass plate was transparent and showed no evidence of extended phase separation, which usually gives an opaque glass. However, it is possible that phase separation is present in the glass at submicrometer or nanometric lengths as it is known for these compositions.[22]

2.2. Poling. In all experiments reported here, thermal poling was performed under nitrogen atmosphere. Glass samples were heated from room temperature to the poling temperature of 300 °C at a rate of 20 °C/min. After 10 min at that temperature, an electric field of 3 kV was applied for a poling time of 30 min. The applied dc bias was removed once the sample had returned to room temperature, which took approximately 20 min.

2.3. Spectroscopy. Micro-Raman and micro-SHG measurements were recorded in backscattering mode on a modified micro-Raman spectrometer HR800 (Horiba/Jobin Yvon). A continuous wave laser operating at 532 nm is used for Raman and a picosecond pulsed laser at 1064 nm is used for micro-SHG measurements. Typical resolution used for Raman is 2.5 cm^{-1}. Measurements of the SHG response were performed using a doughnut radial polarization geometry to probe the electric field in the z-direction (perpendicular to the surface). This particular polarization was obtained by a polarization converter from Arcoptix. The use of a confocal microscope and a motorized (X,Y,Z) stage enables three-dimensional (3D) mapping. The objective used was a 50× with a numerical aperture of 0.42 from Mitutoyo allowing for a resolution in the $X-Y$ plane of 1 and 3 μm in the Z-direction for Raman measurements. Note the resolution in the three directions during μ-SHG mapping is naturally improved as a two-photon excitation process is involved.

IR spectra were recorded on a Vertex 70 V (Bruker) vacuum spectrometer equipped with a DTGS detector and a MID/FIR range beam splitter. To allow measurements on the glass after poling without contacts with the atmosphere, a glovebag was positioned above the sample chamber of the spectrometer. Vacuum was made in the poling cell after poling and the cell was introduced into the glovebag. The glovebag and the spectrometer were put under vacuum and then filled with nitrogen. The sample was taken out of the cell and placed in the spectrometer filled with nitrogen. The spectra were then recorded under vacuum. Measurements at the surface could hence be made without any contact with ambient air. Infrared spectra in reflection mode were recorded using an external reflection attachment (Graesby, Specac) with a 12° incidence angle.

Microinfrared (μ-IR) mapping of the surface was performed using a PerkinElmer Spotlight 400 spectrometer. Spectra were recorded under air with a resolution of 4 cm^{-1} between 4000 and 750 cm^{-1}. Attenuated total reflectance (ATR) spectra were recorded in air on a Nicolet iS50 FT-IR spectrometer between 400 and 4000 cm^{-1} with a 1 cm^{-1} resolution. The spectra were then corrected to allow a better comparison with IR spectra recorded in reflection mode.

3. RESULTS

3.1. Study of the Poled Glass under Inert Atmosphere. The infrared specular reflection spectra of the glass before and after poling, recorded under vacuum, are presented in Figure 1.

After poling under nitrogen, the sample was placed in the IR spectrometer according to the procedure detailed previously. Spectra have been normalized to the band peaking at 1075 cm^{-1} originating from the asymmetric stretching vibrations of fully linked silicon−oxygen tetrahedra Q^4.[23−25] As can be seen, at lower frequencies a contribution arises at 1050 cm^{-1} associated with the asymmetric stretching vibrational modes of B_4−O−Si. Between 1250 and 1500 cm^{-1}, the asymmetric stretching vibrations of $BØ_3$ groups in rings and nonring configurations can be observed.[26] The band near 910 cm^{-1} can be attributed to the asymmetric stretching vibration of $BØ_4^-$ tetrahedra.[13,26,27] In the region below 900 cm^{-1}, highly coupled

DOI: 10.1021/acs.jpcc.5b07139
J. Phys. Chem. C XXXX, XXX, XXX−XXX

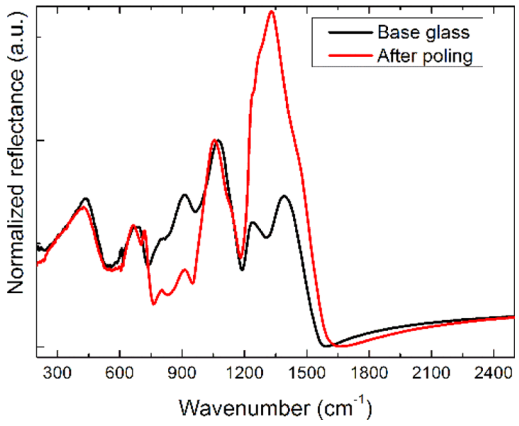

Figure 1. Reflectance spectra of the glass sample before (black) and after poling (red) recorded under vacuum. Both spectra are normalized to the vibrational mode of the Q^4 groups of silica.

deformation modes can be found and attributed to the various constituents of the network such as B−O−B and Si−O−Si bridges or mixed Si−O−B.

Two main differences can be seen to appear between the base glass and the poled sample: (i) a large increase in the band between 1250 and 1500 cm^{-1}, and (ii) a decrease in the intensity of the band between 900 and 1000 cm^{-1}. This change reflects an increase in the $BØ_3$ groups and a decrease of the $BØ_4^-$ units with poling, which can be linked to sodium migration as discussed in this glass system, by Möncke.[13] As can be seen, the bands affiliated with the silica network remain largely unchanged, with slight band shifts to lower wavelength from ∼1075 to ∼1055 cm^{-1} and a shoulder that emerges around 1150 cm^{-1}. As both silica and borate networks are interconnected, following a change in the borate network, a concomitant change in the silica network is expected.

To evaluate the position and strength of the induced second harmonic response, micro-SHG (μ-SHG) mapping was performed on the sample under vacuum and is shown in the schematic in Figure 2. Here, a μ-SHG map was recorded within the x−z plane in the middle of the poled region, as depicted in Figure 2a.

The map in Figure 2b depicts the strength of the SHG signal from the top of the anode side of the specimen (left), into its depth (right) as a function of SHG intensity where the arbitrary units correspond to the integrated area of the SHG peak at 532 nm. The map obtained on a representative poled sample shows that the signal is buried under the anode within the first few micrometers. After the first measurement shown on Figure 2, the sample was kept under vacuum for 2 days and the signal remained stable. Once the impacts of poling on the glass structure and on the static electric field were measured, the sample was taken out of vacuum to evaluate its behavior when exposed to the ambient laboratory atmosphere.

3.2. Study of the Poled Glass in Contact with Air. Once the sample was taken out of the inert atmosphere, it was found to immediately react with air, and several changes were observed to occur at the glass surface. Within an hour, the glass shows a tendency to attract moisture from the atmosphere onto the poled region. The evolution of the second harmonic signal was evaluated during this phenomenon, and the changes with time were noted. The first measurement done within the first minute after opening the chamber showed a strong homogeneous signal buried under the anode, Figure 3a. The maximum is seen within a band nominally 2 μm wide. It is important to keep in mind that for the measurements made under vacuum, as the beam goes through the window of the poling cell, there is a change in numerical aperture. This decreases the confocality of the assembly and the z resolution, which explains the difference in width and in relative intensity between the measurements in vacuum and in air (i.e., results in Figure 2 and Figure 3, respectively). After initial exposure to atmosphere (at time = t_0), a change in intensity of the induced signal is observed. After 7 h (Figure 3b), the SHG signal has lost approximately one-half of its maximum intensity. Figure 3c shows a map recorded 9 h after opening the cell and illustrates the reduction in SHG initially seen in (a). By the end of the day, the SHG signal is 5 times smaller than when the setup was opened.

Figure 4a and b compare IR signatures both within and outside the poled region of the glass' anodic surface and of the ATR spectrum of boric acid. Figure 4c illustrates an optical micrograph of the region below the anode clearly illustrating the poled and unpoled regions, and (d) highlights the corresponding μ-IR map of the same region, spatially illustrating the OH band intensity.

In Figure 4a, the recorded μ-IR spectrum outside the anode is close to the spectrum of the base glass. Modifications appear in the region between 1250 and 1500 cm^{-1} and are due to the various possible configurations of the $BØ_3$ units. On the spectrum taken inside the anode, a large band around 3200 cm^{-1} appears in the minutes following the contact with air. This large band is due to the stretching modes of OH bonds, and the corresponding deformation mode at 1588 cm^{-1} can also be observed. In addition to the signature of water, new contributions appear on the poled glass and can be compared to the spectrum of boric acid. The corrected ATR spectrum of boric acid, shown in part b of the figure, presents a contribution from the B−OH bending mode at 1196 cm^{-1}. B−O stretching modes are found at 883 and 1460 cm^{-1}, while the O−H stretching mode vibrates at 3211 cm^{-1}. Other small contributions are present between 2200 and 2600 cm^{-1} and are combinations of the main bands at smaller wavenumber. As

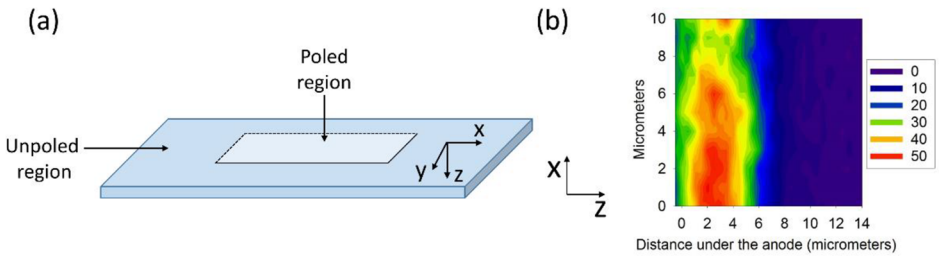

Figure 2. (a) Schematic representation of the mapping principle, and (b) μ-SHG map of a portion of the anode.

DOI: 10.1021/acs.jpcc.5b07139
J. Phys. Chem. C XXXX, XXX, XXX−XXX

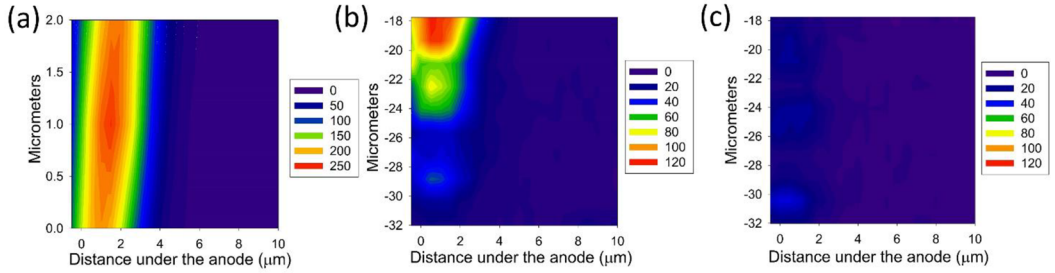

Figure 3. μ-SHG profiles recorded on the sample at different times after opening the poling cell: (a) t_0, (b) t_{0+7h}, and (c) t_{0+9h}.

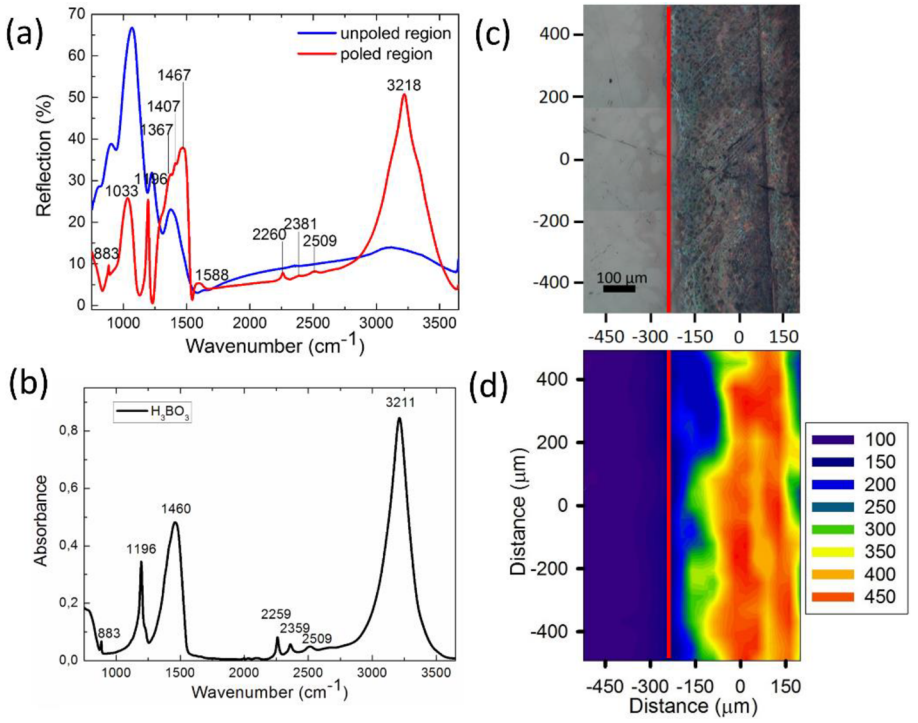

Figure 4. (a) Microinfrared reflectance spectra taken outside and inside the poled region, (b) corrected ATR spectrum of boric acid powder, (c) optical image of the mapped zone in infrared, and (d) infrared map of the OH band (integrated intensity between 2800 and 3600 cm^{-1}) distribution along the frontier between the poled and unpoled regions of the glass, with the red line showing the limit between the unpoled region (left) and poled region (right).

it is observed, the spectrum of the poled region presents bands similar to that found in boric acid, especially at 883, 1196, 1467, 2260, 2381, 2509, and 3218 cm^{-1}, showing the presence of boric acid on the surface.[28,29]

A map of this same region, composed of intensity of the reflection spectra, was then made on a large area (b and c). Here, the area under the band between 2800 and 3600 cm^{-1} was integrated and represented on the map. It can be seen that the OH content increases immediately in the anode area and is relatively homogeneous. A similar map was made inside the anode and showed a homogeneous surface (maximum absorption does not vary more than 10%) over a large area (220 × 220 μm).

To confirm the results obtained in infrared, Raman spectra were recorded at the surface of the anode, as seen in Figure 5. The Raman spectrum of the base glass is shown of part (a) of the figure. The two main bands present on the glass at 770 and 805 cm^{-1} correspond to a triborate group with one $BØ_4^-$ and to $BØ_3$ boroxol rings, respectively.[30−32] The large band in the vicinity of 450 cm^{-1} is due to mixed stretching and bending vibrations from the silicate network.[33] Spectra taken in the poled region do not show large differences in the borate region compared to the IR spectra.

In Figure 5b, the Raman spectrum of boric acid and the polarized spectra of the anode surface measured in both VV and VH polarization configurations (VV and VH notations correspond, respectively, to vertical incident polarization and vertical or horizontal analyzed polarization) after water attraction are presented. Here, new contributions to the glass' spectrum can be seen. The VH polarized Raman spectrum allows one to minimize the portion of the spectrum due to the glass network, preponderant with the VV polarization. As can be seen, six new contributions appear in the spectrum and coincide to those bands seen in boric acid. The peak active at 500 cm^{-1} corresponds to the bending mode of O−B−O bounds. A contribution at 880 cm^{-1} is due to the B−O stretching vibrational mode. Around 1172 cm^{-1}, the bending mode of B−OH bounds is Raman active. The B−O stretching mode can be found around 1384 cm^{-1}. Finally, two contributions are found at higher wavenumbers, 3165 and 3251 cm^{-1}, both corresponding to the O−H stretching vibrational mode.[28,29] Figure 5c and d shows a map of the

DOI: 10.1021/acs.jpcc.5b07139
J. Phys. Chem. C XXXX, XXX, XXX−XXX

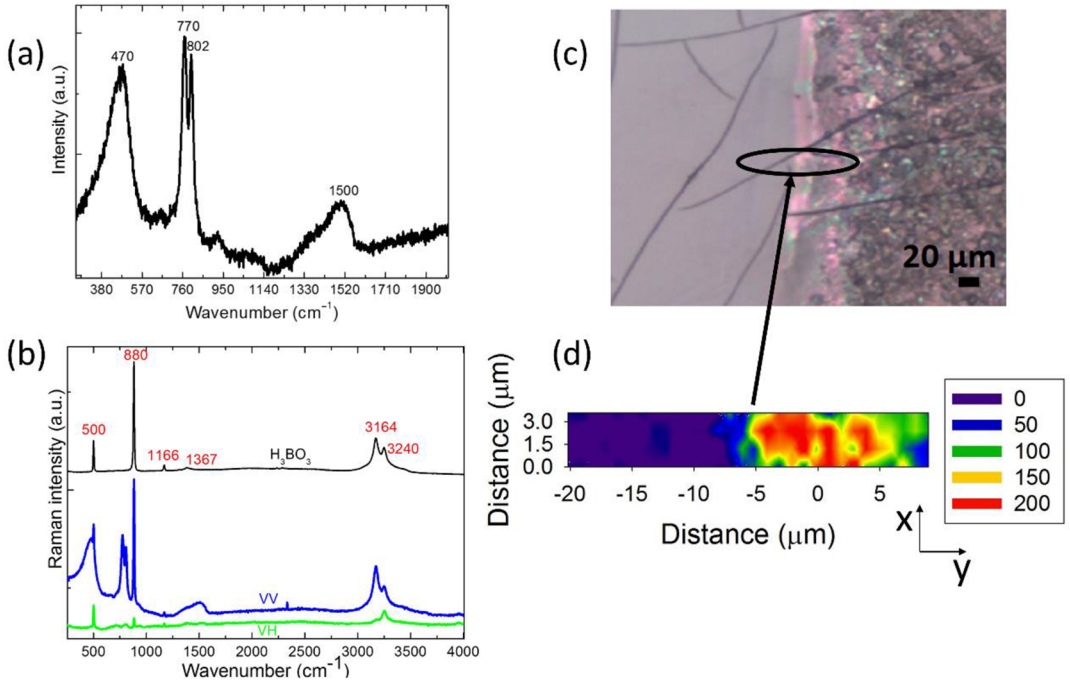

Figure 5. (a) Raman spectrum of the base glass, (b) Raman spectra of boric acid (black) and the surface of the glass in VV (vertical incident polarization−vertical analyzed polarization) and VH (vertical incident polarization−horizontal analyzed polarization) polarization inside the poled region, (c) optical image of the surface, and (d) Raman map of the circled area presenting the intensity distribution of the band at 880 cm^{-1} of boric acid.

interface between the poled region and the rest of the glass. The map shows the intensity of the integrated band at 880 cm^{-1} of the boric acid. Outside the glass, the spectrum of the base glass is obtained, and the spectrum of the glass plus the contribution of boric acid is obtained in the anodic region. The obtained map matches that previously shown in infrared but allows for a better spatial resolution (less than a micrometer, in the *XY* plane). It can be seen that moisture present at the surface is only localized to the anodic surface with a sharp contrast between the poled and unpoled zones.

To evaluate if this surface adsorption could be reversed, the behavior of the moisture-containing glass surface under vacuum was then studied to observe if the OH- rich layer could be removed.

Figure 6 illustrates the infrared spectra recorded following water attraction at the surface and upon re-exposing this surface to vacuum. As noted above, when the poled sample is placed in atmosphere, a large water band at 3250 cm^{-1} appears. The band of the $BØ_3$ units that appeared on Figure 1 has profoundly changed and is now smaller. Moreover, the signature of boric acid can be seen similarly to the spectrum in Figure 4. When this sample is then returned to the vacuum environment, the water band is almost entirely removed after a night. Several regions should be highlighted on the spectrum: (i) the broad peak at 500 cm^{-1} stayed the same over the period of time exposed to vacuum, (ii) the band of the $BØ_3$ units between 1250 and 1500 cm^{-1} changed drastically and went back to a structure closer to the base glass with two separated bands, and (iii) the bands associated with $BØ_4^-$ located near 910 cm^{-1} also diminished.

Raman spectra as well as optical images recorded while the glass was held under vacuum are shown in Figure 7.

As can be seen, the surface coverage of the adsorbed moisture layer decreases rapidly under vacuum. On the Raman

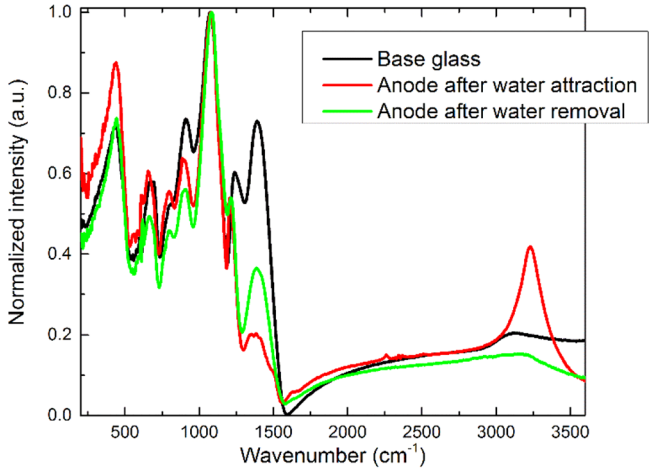

Figure 6. Infrared spectra of the glass: evolution of the structure after poling.

spectra, it can be observed that peaks of the boric acid decrease with the removal of the moisture from the surface. In Figure 7, the time between a and c is 14 h under a primary vacuum. Here, the Raman peaks of the boric acid are finally all gone on the last picture, and the surface of the glass returns to the surface similar to that of the unexposed region.

4. DISCUSSION

4.1. Structure of the Base Glass. Before discussing rearrangements taking place in the glass during poling, it is necessary to have an understanding of the structure of the matrix prior to poling treatment. Sodium borosilicate glasses tend to phase separate;[21] hence the glass can be seen as formed of a silica-rich phase and of a phase close to a binary sodium

DOI: 10.1021/acs.jpcc.5b07139
J. Phys. Chem. C XXXX, XXX, XXX−XXX

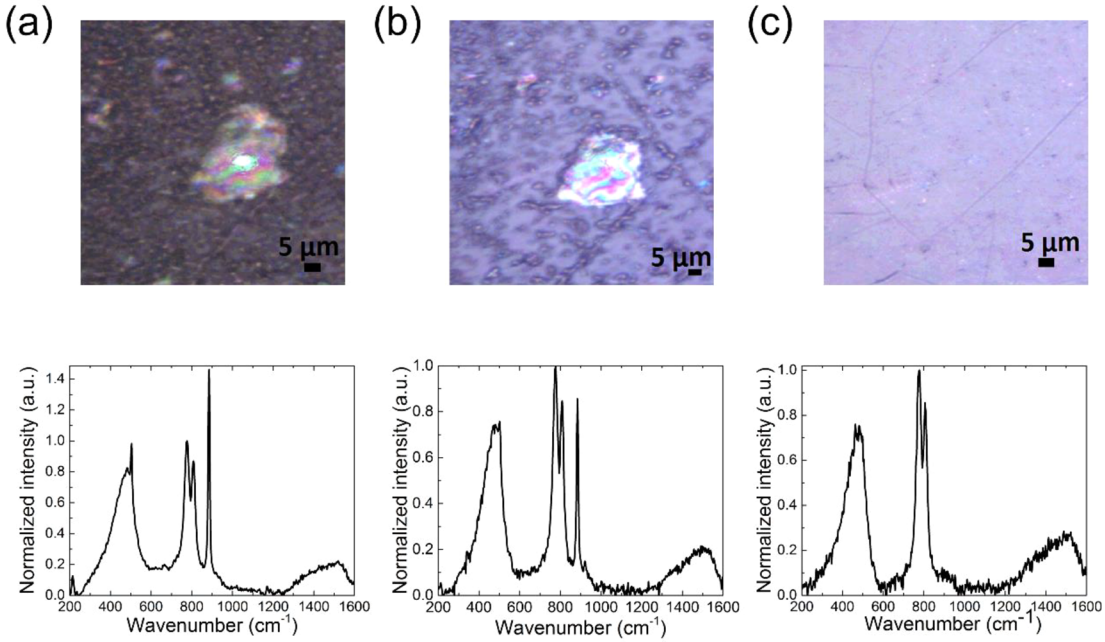

Figure 7. Optical micrograph images of glass surface (top) and Raman spectra (bottom) of glass surface recorded under vacuum, at times (a) t_0, (b) $t_{0+20min}$, and (c) t_{0+14h}.

borate glass. The infrared reflectance spectrum on Figure 1 shows that the silica network is fully reticulated as only one contribution from the asymmetric stretching vibration of the Q^4 tetrahedra, $SiØ_4$, is seen. This is confirmed by the absence of the band at 1100 cm^{-1} from the stretching vibration of $Si-O^-$ in Q^3 species on the Raman spectrum of the base glass, Figure 5a. Hence, all of the sodium added to the composition is going with the borate network to form 4-coordinated boron tetrahedra. The composition of the base glass shows that one sodium is available for five boron, allowing for the formation of one 4-coordinated, $BØ_4^-$, boron for four 3-coordinated boron, $BØ_3$, the ratio of which corresponds to the pentaborate composition (two boroxol rings connected by a boron tetrahedron). This is confirmed by comparison with spectra from binary lithium−borate glasses close to the pentaborate composition. For both studies, spectral similarities can be clearly noticed:[27] (i) the large band of the $BØ_3$ has two components around 1250 and 1390 cm^{-1}; and (ii) the $BØ_4^-$ contribution gives two bands, one around 940 cm^{-1}, along with one around 1080 cm^{-1}, both partially hidden by the silica network. The boron-rich phase of our base glass can thus be seen as mostly formed of pentaborate groups.

Similarly, the Raman spectrum can be compared to Raman spectra from ternary alkali borosilicate glasses in the literature.[13,26,31,33] The presence of alkali in the glass matrix, playing the role of charge compensator, is accompanied by new contribution around 770 cm^{-1} from negatively charged $BØ_4^-$ tetrahedra, in addition to the 806 cm^{-1} contribution from $BØ_3$ units.[32] Those two bands are found in the spectrum of the base glass, showing the presence of those two entities. The ratio of the two bands is directly correlated to the amount of alkali in the matrix acting as charge compensators for the $BØ_4^-$ tetrahedra. Raman spectra of sodium borosilicate in the literature show band intensity similar to Figure 5 for a ratio of sodium to boron close to 0.2.[13,26,31]

4.2. Impact of Thermal Poling on Structure and Electric Field. Thermal poling impacts the glass by creating a space charge following cation departure from the near-anode surface and necessitates charge rearrangements. Under open electrode conditions, cation departure from the subanodic layer is compensated by the injection of positive species from the surrounding atmosphere (mostly H^+ and H_3O^+) and by reticulation of the network.[34−36] The poling in this study is done under nitrogen to meet blocking electrode conditions and to prevent any injections. The results obtained show that the poling was indeed performed under blocking conditions. Infrared reflectance spectra recorded after poling, and not presented here, showed no signature of water injection in the glass. In Figure 1, a large increase of the $BØ_3$ units is accompanied by a decrease of $BØ_4^-$ tetrahedra, which confirms that after sodium departure, the borate network reorganizes. The reflectance activity in the region between 1190 and 1580 cm^{-1} goes from two distinct bands to one large band. This is typical of pure B_2O_3 glasses only made of $BØ_3$ units in boroxol rings and independent triangles. In those glasses, no contribution to the reflectance spectra is found between 800 and 1200 cm^{-1}.[27] In the poled glass, a small contribution is found at those wavenumbers and is due to the unmodified bulk glass. In the subanodic region, the network has been changed from pentaborate groups to a B_2O_3-like structure. The rearrangement taking place in this study is in agreement with a previous report by Möncke et al.[13] who studied structural changes in borosilicate glasses of compositions on the boric oxide anomaly. They were able to identify the structural changes associated with the sodium departure from the subanodic layer and to link it to the following process:

$$NaBØ_4 \rightarrow Na^+ + BØ_3 + 1/2O^{2-}$$

The same process takes place in our experiment. In addition to structural rearrangements, a space charge is created in the near-surface area at the anode. This static electric field breaks the centrosymmetry of the glass allowing for second-order nonlinear properties such as second harmonic generation (SHG). Micro-SHG is used to find the position and intensity of

DOI: 10.1021/acs.jpcc.5b07139
J. Phys. Chem. C XXXX, XXX, XXX−XXX

the electric field of Figure 2. As stated in the Results, the active layer is approximately 2 μm thick in the first micrometers beneath the surface of the glass. This result is in good agreement with previous studies of poling realized in blocking anode conditions,[5] contrary to poling in open anode where the nonlinear layer is wider.[5]

We showed that the structural rearrangements taking place in this study could be explained quite easily by the departure of sodium. However, the nature of the negative charge carriers involved during the poling process to compensate the cation depletion is more complex. Our study confirms indirectly the important role of oxygen, but no conclusion can be done on the respective role of electronic and/or anionic contributions linked to the structural rearrangements observed for this borosilicate polarized glassy system.[15,34−39] Nevertheless, the poling performed on the glass allows the creation of the expected structure beneath the anode associated with a static electric field, the intensity and thickness values of which are in agreement with a blocking anode configuration. The newly formed charged borate structure was kept under vacuum for several days, and both the new structure and the induced static electric field remain stable.

4.3. Reactivity of the Glass in Atmosphere. As mentioned in the Results, once the sample is taken out of the vacuum, the poled region presents a strong reactivity with the atmosphere. As shown in Figures 4 and 6, a large OH band appears on the infrared spectra of the glass highlighting the strong affinity of the poled region toward water. The surface coverage of the poled zone with water is almost total as seen on the optical images of Figure 7a and with micro-IR and micro-Raman spectroscopies. The affinity of the poled region to water is attributed to the new structure with more boroxol rings, which are highly hygroscopic. Moreover, the presence of the static electric field inside the glass might further enhance this effect from electrostatic interaction.[40,41]When water is present at the surface of the glass, it reacts with the glass matrix; the process involved is a typical glass leaching process. The glass is boron-rich and locally close to a pure B_2O_3 glass after poling; the most present bonds at the glass surface are B−O−B bonds. Water reacts with those bonds to form B−OH bonds.[42] As the reaction proceeds, boron is progressively released from the glass matrix and boric acid H_3BO_3 forms in the water layer as the good correlation between the corrected ATR spectrum of boric acid and the infrared spectrum of the glass shows. The slight difference between the corrected ATR spectrum and the poled region can be linked to the fact that the boric acid on the glass surface is in the presence of water while the ATR spectrum was recorded on a powder. The presence of boric acid is confirmed by Raman measurements from Figure 5 where distinct peaks of boric acid in addition to the Raman spectrum of the base glass are present. Raman mapping of the frontier between the poled and unpoled region shows boric acid only on the anode with a sharp resolution, smaller than a micrometer. The Raman spectrum of dissolved boric acid is known to be similar to that of boric acid powder;[43] the good correlation between the two allows us to confirm without doubts that boric acid is truly forming. Moreover, the ratio of the 880 cm^{-1} band to the 3400 cm^{-1} band (originating from molecular water) is directly linked to the concentration of boric acid in the solution and has been previously used to estimate the concentration of boric acid in a solution.[43] If the same methodology is used on our results to estimate the concentration of boric acid in the solution at the surface of the glass, a concentration up to 20 wt % can be found. In addition to the leaching process, the presence of water at the surface is accompanied by a decrease of the SHG signal observed in μ-SHG measurements, Figure 3. The SHG intensity is up to 10 times lower by the end of the day as observed in Figure 3. The decrease in SHG intensity is directly linked to the progressive destruction of the modified layer in the anodic region. The mechanism taking place on the poled zone in atmosphere can be summarized as follows: (i) in the presence of moisture, the charged borate structure attracts water at the surface, (ii) once water is on the surface, it reacts with the borate network to form boric acid, and (iii) as water reacts with the sample, the SHG intensity decays over the day.

When this OH-rich layer is formed and has reacted with the glass to form H_3BO_3, it is possible to remove it by placing the sample under vacuum. As observed in Figure 7, surface coverage decreases simultaneously with the disappearance of the Raman signature of boric acid. After pumping, boric acid and water are no more present at the surface. The boric acid solution on the surface is removed by evaporation. Boric acid in solution is volatile and can be evaporated upon heating.[43,44] It is another proof that boric acid formed at the surface is not bonded to the glass network. From the infrared reflectance spectrum after the OH-rich layer has been removed, it can be observed (Figure 6) that the structure does not recover its original state. The signature of the $BØ_3$ units is smaller, with one contribution, while the $BØ_4^-$ signature at lower frequencies is not back to the intensity of the unpoled glass. The boron-rich phase has been partially removed from the glass. When the OH-rich layer is taken out of the surface, the glass still presents an interesting affinity toward water. Contact angle measurements have been performed and showed a near to perfect wettability of the poled zone. The change of surface wettability is not comparable to the effects found by Ziemath et al.[45] at the anodic surface of thermally poled soda-lime float glasses, where the surface was hydrophobic. The impact of thermal poling on wettability properties is dependent on glass compositions and strength of the induced static electric field at the glass−air interface. Further studies are needed to control this effect as a function of poling conditions and glass composition. Nevertheless, it could give the possibility to confine size-controlled water droplets at the surface of the poled area, which present a real interest as potential microreactors.

5. CONCLUSION

This study aimed to understand the impact of poling and its ability to locally change the reactivity and structure of borosilicate glass surfaces. We have shown that by precisely controlling the parameters of the thermal poling process and carefully choosing the glass composition, it is possible to create a modified borate structure made of boroxol rings $BØ_3$, accompanied by a strong electric field below the glass' surface. While the sample is kept under vacuum, the structure and the electric field are stable over time. However, once the sample is placed in air, the combined effect of both the electric field and the structural change permits one to attract water locally on the glass surface. The glass can be seen as made of two networks: the silica network, where the skeleton of the matrix is not impacted by the treatment or by water attraction, while the borate network is the center of reactivity for reactions involving water to take place. Water reacts with the borate network, forming boric acid. This OH-rich layer remains stable over time and can be removed by simple vacuum. The set of

DOI: 10.1021/acs.jpcc.5b07139
J. Phys. Chem. C XXXX, XXX, XXX−XXX

characterization technique used in this study confirmed our hypothesis on imparting structural changes through poling with a concurrent creation of a frozen-in electric field. Last, following water removal, contact angle measurements were performed and showed a good wettability of the surface, with nearly total wettability. This resulted in a strong contrast in wettability between the poled and unpoled regions and proof that good spatial confinement of water is possible at the surface. This opens possibilities for future applications where a substrate comprised of multiple poled zones, with enhanced reactivity, could be used as receptacles for molecules and their interaction with targeted chemistries or environments.

AUTHOR INFORMATION

Corresponding Author

*E-mail: m.dussauze@ism.u-bordeaux1.fr.

Notes

The authors declare no competing financial interest.

ACKNOWLEDGMENTS

This study has been carried out with financial support from the French State, managed by the French National Research Agency (ANR) in the frame of "the Investments for the future" Programme IdEx Bordeaux – LAPHIA (ANR-10-IDEX-03-02), and the French Aquitaine region [Grant 20121101025]. A.L. and K.R. acknowledge support of the National Science Foundation, award no. DMR-1308946.

REFERENCES

(1) Myers, R. A.; Mukherjee, N.; Brueck, S. R. J. Large Second-Order Nonlinearity in Poled Fused Silica. *Opt. Lett.* **1991**, *16*, 1732−1734.

(2) Kazansky, P. G.; Russel, P. S. J. Thermally Poled Glass: Frozen-in Electric Field Or Oriented Dipoles? *Opt. Commun.* **1994**, *110*, 611−614.

(3) Mukherjee, N.; Myers, R. A.; Brueck, S. R. J. Dynamics of Second-Harmonic Generation in Fused Silica. *J. Opt. Soc. Am. B* **1994**, *11*, 665−669.

(4) Alley, T. G.; Brueck, S. R. J.; Wiedenbeck, M. Secondary Ion Mass Spectrometry Study of Space-Charge Formation in Thermally Poled Fused Silica. *J. Appl. Phys.* **1999**, *86*, 6634−6640.

(5) Dussauze, M.; Rodriguez, V.; Lipovskii, A.; Petrov, M.; Smith, C.; Richardson, K.; Cardinal, T.; Fargin, E.; Kamitsos, E. I. How does Thermal Poling Affect the Structure of Soda-Lime Glass? *J. Phys. Chem. C* **2010**, *114*, 12754−12759.

(6) Dussauze, M.; Cremoux, T.; Adamietz, F.; Rodriguez, V.; Fargin, E.; Yang, G.; Cardinal, T. Thermal Poling of Optical Glasses: Mechanisms and Second-Order Optical Properties. *Int. J. Appl. Glass Sci.* **2012**, *3*, 309−320.

(7) Guimbretiere, G.; Dussauze, M.; Rodriguez, V.; Kamitsos, E. I. Correlation between Second-Order Optical Response and Structure in Thermally Poled Sodium Niobium-Germanate Glass. *Appl. Phys. Lett.* **2010**, *97*, 171103.

(8) Dussauze, M.; Fargin, E.; Malakho, A.; Rodriguez, V.; Buffeteau, T.; Adamietz, F. Correlation of Large SHG Responses with Structural Characterization in Borophosphate Niobium Glasses. *Opt. Mater.* **2006**, *28*, 1417−1422.

(9) Dussauze, M.; Kamitsos, E. I.; Fargin, E.; Rodriguez, V. Structural Rearrangements and Second-Order Optical Response in the Space Charge Layer of Thermally Poled Sodium-Niobium Borophosphate Glasses. *J. Phys. Chem. C* **2007**, *111*, 14560−14566.

(10) Dussauze, M.; Fargin, E.; Rodriguez, V.; Malakho, A.; Kamitsos, E. Enhanced Raman Scattering in Thermally Poled Sodium-Niobium Borophosphate Glasses. *J. Appl. Phys.* **2007**, *101*, 083532.

(11) Smith, N. J.; Pantano, C. G. Structural and Compositional Modification of a Barium Boroaluminosilicate Glass Surface by Thermal Poling. *Appl. Phys. A: Mater. Sci. Process.* **2014**, *116*, 529−543.

(12) Dussauze, M.; Rodriguez, V.; Velli, L.; Varsamis, C. P. E.; Kamitsos, E. I. Polarization Mechanisms and Structural Rearrangements in Thermally Poled Sodium-Alumino Phosphate Glasses. *J. Appl. Phys.* **2010**, *107*, 043505.

(13) Möncke, D.; Dussauze, M.; Kamitsos, E. I.; Varsamis, C. P. E.; Ehrt, D. Thermal Poling Induced Structural Changes in Sodium Borosilicate Glasses. *Phys. Chem. Glasses-B* **2009**, *50*, 229−235.

(14) Hench, L. L.; Splinter, R. J.; Allen, W. C.; Greenlee, T. K. Bonding Mechanisms at the Interface of Ceramic Prosthetic Materials. *J. Biomed. Mater. Res.* **1971**, *5*, 117−141.

(15) Mariappan, C. R.; Roling, B. Mechanism and Kinetics of Na+ Ion Depletion Under the Anode during Electro-Thermal Poling of a Bioactive Glass. *J. Non-Cryst. Solids* **2010**, *356*, 720−724.

(16) Yamashita, K.; Oikawa, N.; Umegaki, T. Acceleration and Deceleration of Bone-Like Crystal Growth on Ceramic Hydroxyapatite by Electric Poling. *Chem. Mater.* **1996**, *8*, 2697−2700.

(17) Obata, A.; Nakamura, S.; Moriyoshi, Y.; Yamashita, K. Electrical Polarization of Bioactive Glass and Assessment of their in Vitro Apatite Deposition. *J. Biomed. Mater. Res.* **2003**, *67*, 413−420.

(18) Nakamura, S.; Kobayashi, T.; Nakamura, M.; Itoh, S.; Yamashita, K. Electrostatic Surface Charge Acceleration of Bone Ingrowth of Porous Hydroxyapatite/ß-Tricalcium Phosphate Ceramics. *J. Biomed. Mater. Res., Part A* **2010**, *92*, 267−275.

(19) Mariappan, C. R.; Roling, B. Investigation of Bioglass-Electrode Interfaces After Thermal Poling. *Solid State Ionics* **2008**, *179*, 671−677.

(20) Mariappan, C. R.; Yunos, D. M.; Boccaccini, A. R.; Roling, B. Bioactivity of Electro-Thermally Poled Bioactive Silicate Glass. *Acta Biomater.* **2009**, *5*, 1274−1283.

(21) Shelby, J. E.; Lopes, M. *Introduction to Glass Science and Technology*; The Royal Society of Chemistry: UK, 2005; 292 pp.

(22) Ehrt, D.; Keding, R. Electrical Conductivity and Viscosity of Borosilicate Glasses and Melts. *Phys. Chem. Glasses-B* **2009**, *50*, 165−171.

(23) Tenney, A. S.; Wong, J. Vibrational Spectra of Vapor-Deposited Binary Borosilicate Glasses. *J. Chem. Phys.* **1972**, *56*, 5516−5523.

(24) Bell, R. J.; Carnevale, A.; Kurkjian, C. R.; Peterson, G. E. Structure and Phonon Spectra of SiO2, B2O3 and Mixed SiO2B2O3 Glasses. *J. Non-Cryst. Solids* **1980**, *35−36*, 1185−1190.

(25) Kamitsos, E. I.; Patsis, A. P.; Kordas, G. Infrared-Reflectance Spectra of Heat-Treated Sol-Gel-Derived Silica. *Phys. Rev. B: Condens. Matter Mater. Phys.* **1993**, *48*, 12499−12505.

(26) Möncke, D.; Ehrt, D.; Varsamis, C.-E.; Kamitsos, E. I.; Kalampounias, A. G. Thermal History of a Low Alkali Borosilicate Glass Probed by Infrared and Raman Spectroscopy. *Glass Technol.-Part A* **2006**, *47*, 133−137.

(27) Kamitsos, E. I.; Patsis, A. P.; Karakassides, M. A.; Chryssikos, G. D. Infrared Reflectance Spectra of Lithium Borate Glasses. *J. Non-Cryst. Solids* **1990**, *126*, 52−67.

(28) Bethell, D. E.; Sheppard, N. The Infra-Red Spectrum and Structure of Boric Acid. *Trans. Faraday Soc.* **1955**, *51*, 9−15−15.

(29) Krishnan, K. The Raman Spectrum of Boric Acid. *Proc. Indian Acad. Sci., Sect. A* **1963**, *57*, 103−108.

(30) Konijnendijk, W. L. *The Structure of Borosilicate Glasses*; Technische Hogeschool: Eindhoven, 1975.

(31) Furukawa, T.; Fox, K. E.; White, W. B. Raman Spectroscopic Investigation of the Structure of Silicate Glasses. III. Raman Intensities and Structural Units in Sodium Silicate Glasses. *J. Chem. Phys.* **1981**, *75*, 3226−3237.

(32) Kamitsos, E. I.; Chryssikos, G. D.; Karakassides, M. A. New Insights into the Structure of Alkali Borate Glasses. *J. Non-Cryst. Solids* **1990**, *123*, 283−285.

(33) Brethous, J.; Levasseur, A.; Villeneuve, G.; Echegut, P.; Hagenmuller, P.; Couzi, M. Etudes Par Spectroscopie Raman Et Par RMN Des Verres Du Système B2O3 SiO2 Li2O. *J. Solid State Chem.* **1981**, *39*, 199−208.

(34) Carlson, D. E.; Hang, K. W.; Stockdale, G. F. Electrode "Polarization" in Alkali-Containing Glasses. *J. Am. Ceram. Soc.* **1972**, *55*, 337−341.

DOI: 10.1021/acs.jpcc.5b07139
J. Phys. Chem. C XXXX, XXX, XXX−XXX

(35) Carlson, D. E.; Hang, K. W.; Stockdale, G. F. Ion Depletion of Glass at a Blocking Anode - 1, 2. *J. Am. Ceram. Soc.* **1974**, *57*, 295−300.
(36) Carlson, D. E. Anodic Proton Injection in Glasses. *J. Am. Ceram. Soc.* **1974**, *57*, 461−466.
(37) Krieger, U. K.; Lanford, W. A. Field Assisted Transport of Na+ Ions, Ca2+ Ions and Electrons in Commercial Soda-Lime Glass I: Experimental. *J. Non-Cryst. Solids* **1988**, *102*, 50−61.
(38) Lipovskii, A. A.; Melehin, V. G.; Petrov, M. I.; Svirko, Y. P.; Zhurikhina, V. V. Bleaching Versus Poling: Comparison of Electric Field Induced Phenomena in Glasses and Glass-Metal Nanocomposites. *J. Appl. Phys.* **2011**, *109*, 011101.
(39) Cremoux, T.; Dussauze, M.; Fargin, E.; Cardinal, T.; Talaga, D.; Adamietz, F.; Rodriguez, V. Trapped Molecular and Ionic Species in Poled Borosilicate Glasses: Toward a Rationalized Description of Thermal Poling in Glasses. *J. Phys. Chem. C* **2014**, *118*, 3716−3723.
(40) Decher, G. Fuzzy Nanoassemblies: Toward Layered Polymeric Multicomposites. *Science* **1997**, *277*, 1232−1237.
(41) Palleau, E.; Sangeetha, N. M.; Viau, G.; Marty, J.; Ressier, L. Coulomb Force Directed Single and Binary Assembly of Nanoparticles from Aqueous Dispersions by AFM Nanoxerography. *ACS Nano* **2011**, *5*, 4228−4235.
(42) Zapol, P.; He, H.; Kwon, K. D.; Criscenti, L. J. First-Principles Study of Hydrolysis Reaction Barriers in a Sodium Borosilicate Glass. *Int. J. Appl. Glass Sci.* **2013**, *4*, 395−407.
(43) Thomas, R. Determination of the H3BO3 Concentration in Fluid and Melt Inclusions in Granite Pegmatites by Laser Raman Microprobe Spectroscopy. *Am. Mineral.* **2002**, *87*, 56−68.
(44) Böhlke, S.; Schuster, C.; Hurtado, A. About the Volatility of Boron in Aqueous Solutions of Borates with Vapour in Relevance to BWR-Reactors. *International Conference on the Physics of Reactors*; 2008; Vol. *4*, pp 3089−3096.
(45) Ziemath, E. C.; Araújo, V. D.; Escanhoela, C. A. Compositional and Structural Changes at the Anodic Surface of Thermally Poled Soda-Lime Float Glass. *J. Appl. Phys.* **2008**, *104*, 054912.

DOI: 10.1021/acs.jpcc.5b07139
J. Phys. Chem. C XXXX, XXX, XXX−XXX